

MetroLab PDI Measurement System Commissioning Detail

K. Baggett, M. Beck, T. Hiatt and K. Sullivan
Thomas Jefferson National Accelerator Facility, Newport News, Virginia 23606

1 Introduction

This paper will discuss a series of system tests that have been conducted on the MetroLab PDI multipole measurement system. The PDI system will replace the existing CAMAC multipole measurement system in the Magnet Measurement Facility. These tests were conducted for commissioning purposes and are intended to quantify the repeatability of the PDI system under various conditions including:

1. Quantifying the repeatability of the quadrupole term of a reference signal simulating 5 continuous forward probe rotations when
 - a. The reference signal is plugged directly into the PDI unit
 - b. The reference signal is plugged into each of the three measurement probe coil locations
2. Quantifying the repeatability of the quadrupole term of a reference signal simulating 5 discrete forward rotations (averaged) when
 - a. The reference signal is plugged into each of the three measurement probe coil locations
3. Quantifying the repeatability of the quadrupole term at a single current for each rotating coil probe
 - a. P1A – 1 inch Halbach style probe
 - b. P1C – 1 inch Single coil probe
 - c. P2A – 2 inch Halbach style probe
 - d. P2B – 2 inch Single coil probe
 - e. P3A – 3 inch Halbach style probe
4. Comparing two signal analysis algorithms for egregious differences
 - a. FFT algorithm from CAMAC code
 - b. FFT algorithm from the National Instruments function library

2 Reference Signal Repeatability

For normal data acquisition operations, the voltage signal from the measurement probe is routed through a series of couplings, cables, and hardware upstream of the PDI unit. An HP 33120A function generator was used in place of the measurement probe to create a +/-300 mV, 1.596 Hz reference voltage signal. The 300 mV amplitude of the reference signal is comparable to the voltage induced in the one inch, single coil probe, P1C, when measuring a QA magnet at 3 amps.

Initial measurements were conducted with a reference signal input directly to the PDI unit, in an effort to quantify the 'best case' repeatability of a simplified system. A comparison was made between averaging five two period cycles, representing five discrete forward rotations of the measurement probe in a quadrupole magnet, and analyzing a single ten period cycle, representing five continuous forward rotations of a

measurement probe in a quadrupole magnet. Both sets of data exhibited short term (less than four hours) reproducibility across measurement sets at or less than 0.015% for the 1.596 Hz, 300 mV reference signal. The setup and results of these measurements are detailed below.

2.1 Function Generator Reference Signal Setup

The signal from an optical trigger was split and used to synch the PDI unit and the function generator as the motor rotated through 360 degrees. The reference signal was set such that one 360 degree rotation of the motor was coincident with two signal periods, simulating the rotation of a measurement probe in a quadrupole magnet. The PDI uses encoder information from the motor to integrate incoming signals; therefore synchronization between the motor and the reference signal was essential. Two hundred data points were collected for a single 360 degree rotation of the motor.

Discrete Forward Rotation

The current method of measuring multipole magnets on the rotating coil stand involves collecting data on the forward, 360 degree, revolution of the measurement probe. The probe rotation is then reversed and data is collected during the reverse 360 degree rotation. The forward and reverse data is averaged, and this process is repeated five times concluding when the five data sets are averaged to represent the magnet induced waveform.

However, for simulation purposes, it is not feasible to average data when simulating a rotating measurement because of the complexity of synchronizing the reference signal to the reverse rotation. Therefore only data collected on a forward rotation will be analyzed. Once five discrete forward rotations had been simulated, the five arrays of data points were averaged and analyzed using an FFT to resolve the harmonic contents of the average wave form.

Continuous Forward Rotation

Continuous probe rotation is a method of data acquisition used at several labs around the country. To accomplish continuous rotation, slip rings are used to allow the measurement probe to rotate multiple times in one direction without the need for reversing.

To simulate continuous rotation, the limit switches were removed from the rotation stand and the encoder position zeroed approximately 45 degrees behind the optical synchronization trigger. A trigger arm attached to the motor shaft caused the optical sensor to fire a TTL signal, triggering the PDI to begin data acquisition and the HP 33120A to begin a ten period burst as the motor rotated through five revolutions. Continuous rotation provided additional zero crossings allowing the FFT function to better resolve the waveform. The PDI collected 1,000 data points during the five rotations before completing data acquisition and transferring the integrated voltage samples to the host computer.

2.2 Continuous Rotation Testing with Reference Signal

Continuous Rotation – Direct PDI Connection

Tests were conducted to quantify the repeatability of simulated continuous probe rotation. As described previously, a single ten period cycle was used to represent the signal induced from five continuous forward rotations of a measurement probe in a quadrupole magnet.

Figure 2.1.1-I, shows the results of the test, where 1,000 individual samples, 200 samples per revolution for five revolutions, were collected during data acquisition. Data sets for 'Run 1', 'Run 2' and 'Run 3' show the averaged quadrupole term from ten independent measurements.

Continuous Rotation – Coil 1 Probe Location

To investigate system noise, the reference signal input was moved from a direct connection on the PDI unit, to the coil 1 input location for the rotating coil probe. From this location the reference signal passed through the entire data acquisition system, a series of twisted pair cables, DIN connectors, a signal chassis box, and a multiplexer before reaching the PDI unit.

Table 2.1.1 II shows the measurement results after the reference signal was moved to the coil 1 location. Data sets for 'Run 1', 'Run 2' and 'Run 3' show the averaged quadrupole term from ten independent measurements. The system repeatability for a given ten run data set was better than 0.02%. However, the maximum spread across the entire thirty measurements comprising these three runs was 0.05%. A contributor to this degradation in repeatability is associated with the signal drift across the three runs. The drift could be associated with environmental factors or small synchronization errors between the function generator burst and motor encoder, causing the PDI unit to integrate different amounts of the reference signal for the individual runs.

5 Continuous Revolutions			
Signal Connected at the PDI Directly -- n = 2 Term			
9/13/2005	QXtst013.fft	QXtst012.fft	QXtst011.fft
10 Measurements per Run	Run 1	Run 2	Run 3
Max (uV*Sec)	30950.42	30950.67	30950.13
Min (uV*Sec)	30948.94	30948.70	30949.17
Difference (uV*Sec)	1.48	1.97	0.96
Deviation (%)	0.005%	0.006%	0.003%
Max Overall (uV*Sec)	30950.67		
Min Overall (uV*Sec)	30948.70		
Amplitude Delta (uV*Sec)	1.97		
3 Run Deviation (%)	0.006%		

Table 2.1.1-I Five Continuous Revolutions

5 Continuous Revolutions			
Signal Connected at Coil 1 Probe Location – n = 2			
9/13/2005	QXtst030.fft	QXtst031.fft	QXtst036.fft
10 Measurements	Run 1	Run 2	Run 3
Max (uV*Sec)	30957.02	30960.27	30967.96
Min (uV*Sec)	30952.36	30958.28	30964.92
Difference (uV*Sec)	4.66	1.99	3.03
Deviation (%)	0.015%	0.006%	0.010%
Max Overall (uV*Sec)	30967.96		
Min Overall (uV*Sec)	30952.36		
Amplitude Delta	15.60		
3 Run Deviation (%)	0.050%		

Table 2.1.1-II Five Continuous Revolutions

Continuous Rotation – All Coil Locations

There are two other coil input locations on the rotating coil stand in addition to the coil 1 location. Each coil location was tested using the continuous rotation method to verify consistency in system repeatability across coil locations. A series of three data sets, consisting of ten separate measurements of the 1.596 Hz reference signal, were taken at each of the other two locations. Figure 2.1.1.I shows the deviation in the quadrupole term from the measurement average, for each of the ten measurements taken in each of three runs, at the three coil location.

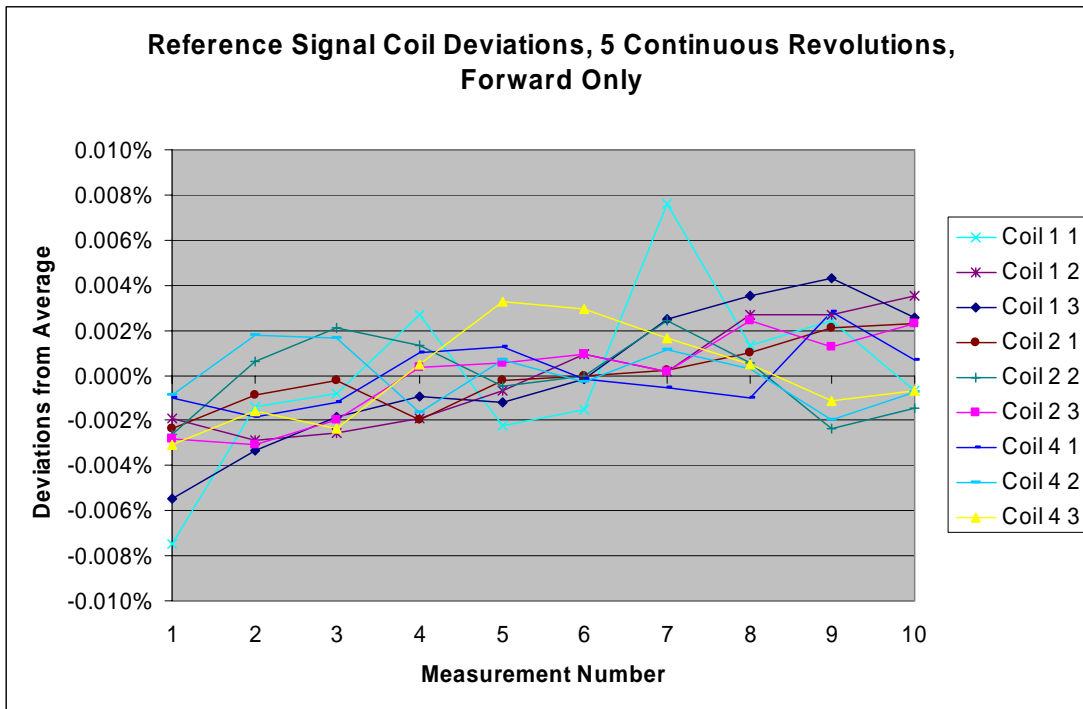


Figure 2.1.1-1 Main harmonic amplitude reproducibility using 5 sequential cycles

2.2.1 2.3 Five Cycle Averaged Rotation Testing with Reference Signal

5 Discrete Forward Rotations Averaged – Coil 1 Probe Location

The reference signal was connected at the coil 1 probe location and measurements were made simulating five individual forward probe rotations. The results of these five rotations were averaged. This process was repeated ten times for ‘Run 1’, ‘Run 2’ and ‘Run 3’ respectively.

Table 2.3-I shows the results from averaging the five forward rotations were slightly degraded in terms of system repeatability for each run when compared to the continuous rotation data. The worst case set of ten measurements, ‘Run 3’, repeated to 0.014%. There was however, less drift in the absolute value of the quadrupole term during the measurements of these three runs when compared to the continuous rotation runs. The maximum spread across the entire set of thirty measurements constituting these runs was 0.019%, a factor of 2.5 better than the system repeatability of the thirty measurements used for the continuous rotation tests.

5 Discrete Forward Rotations Averaged – All Coil Locations

Tests were repeated at the other two coil probe locations. Figure 2.3-II shows the deviation in the quadrupole term from the measurement average, for the ten sets of data taken in each of three runs, at each coil location. This data is slightly noisier than the similar data obtained for the continuous rotation tests.

Five Averaged Revolutions (Forward Only)			
Signal Connected at the Coil 1 Probe Location – n = 2			
10/6/2005	QXtst033.fft	QXtst034.fft	QXtst035.fft
10 Measurements	Run 1	Run 2	Run 3
Max (uV*Sec)	31009.98	31007.99	31010.12
Min (uV*Sec)	31006.30	31004.28	31005.77
Avg (uV*Sec)	31008.54	31006.40	31008.37
Difference (uV*Sec)	3.68	3.72	4.35
Deviation (%)	0.012%	0.012%	0.014%
Max Overall (uV*Sec)	31010.12		
Min Overall (uV*Sec)	31004.28		
Amplitude Delta (uV*Sec)	5.84		
3 Run Deviation (%)	0.019%		

Table 2.2-I Five Averaged Cycles per Revolution

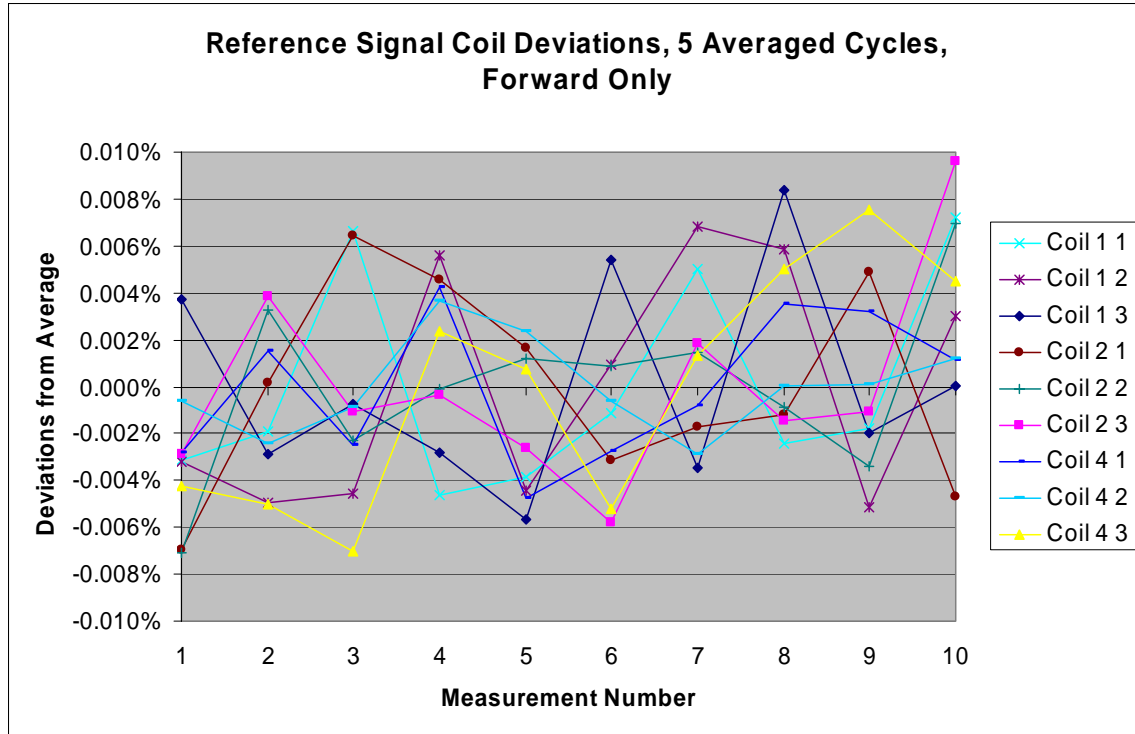


Figure 2.3-II Main harmonic amplitude reproducibility using the average of 5 cycles

3 Signal Analysis Algorithm Comparison

During the multipole measurement process, the PDI system integrates voltage samples according to:

$$\int_0^t V(t)dt = \Phi(0) - \Phi(\theta),$$

for each coil rotation. These integrated values ($V \cdot S$) are then transferred to the control computer. To understand the harmonic content of the waveform, an FFT algorithm is used to obtain the normal and skew field components **before** performing amplitude and phase calculations for the desired harmonics.

The CAMAC data acquisition software used an algorithm developed at Jefferson Lab to calculate and normalize the voltage integrals before computing the amplitude and phase of each harmonic. The PDI software uses a LabWindows/CVI library function to perform an FFT on the data.

To verify that the PDI and CAMAC FFT algorithms, and subsequent amplitude and phase calculations, were consistent, the CAMAC FFT function was transferred into the PDI code and refactored to work with the PDI array structures and indexing. Both algorithms use similar code to compute the amplitude of each harmonic but the phase angle computations were slightly differently. Two data runs, one that was used to

process the integrated voltage samples using the CAMAC algorithm and one used to process the samples using the PDI algorithm, were taken to collect information for the comparison. The magnet was cycled and set to five amps prior to the first run and was left at five amps through the duration of the second run. Data was taken and the phase angles were computed using both algorithms. Results of the analysis showed reasonably consistent phase angles at each harmonic. Table 3-1 shows phase angles using both algorithms for the specified harmonic. Table 3-II compares the amplitudes of the two FFT methods from the same two runs.

CAMAC FFT Algorithm Results (degrees)								
Avg Curr	n = 1	n = 2	n = 3	n = 4	n = 5	n = 6	n = 7	n = 8
5.0	-133.59	-61.07	37.68	-28.78	12.39	-27.45	-0.80	-13.46
5.0	-134.03	-61.08	37.84	-31.71	24.22	-23.46	-15.53	-13.73
5.0	-132.90	-61.07	36.92	-30.24	16.29	-24.90	3.87	-12.04
5.0	-134.18	-61.09	38.08	-33.57	24.63	-26.94	5.19	-15.53
5.0	-134.75	-61.10	38.96	-31.15	26.34	-25.53	15.56	-17.08
PDI FFT Algorithm Results (degrees)								
Avg Curr	n = 1	n = 2	n = 3	n = 4	n = 5	n = 6	n = 7	n = 8
5.0	-133.88	-61.09	37.49	-34.42	20.98	-29.60	2.06	-10.11
5.0	-134.22	-61.09	38.29	-31.77	20.39	-27.50	2.48	-17.37
5.0	-134.60	-61.07	38.49	-24.58	25.95	27.58	2.84	-20.18
5.0	-133.60	-61.08	37.92	-25.76	20.19	-7.52	0.09	-13.28
5.0	-133.61	-61.08	37.69	-28.09	22.45	14.01	-5.20	-13.25

CAMAC FFT Algorithm Results (degrees) (cont.)								
n = 9	n = 10	n = 11	n = 12	n = 13	n = 14	n = 15	n = 16	n = 17
-14.19	-0.17	-12.31	-1.23	-8.91	0.78	-7.02	6.35	-1.43
17.83	-3.26	-12.21	-4.43	-12.74	-8.25	8.38	3.82	-6.47
16.35	0.92	-12.57	-0.28	-6.48	-11.95	-2.47	-8.11	-0.76
17.46	12.22	-13.78	0.15	-10.99	-7.00	10.20	6.67	-4.54
18.41	-14.10	-13.93	10.42	-12.48	-4.20	-11.93	10.21	-5.94
PDI FFT Algorithm Results (degrees) (cont.)								
n = 9	n = 10	n = 11	n = 12	n = 13	n = 14	n = 15	n = 16	n = 17
-16.71	5.76	14.86	4.14	-10.11	0.53	11.83	8.75	-1.66
-19.55	14.84	-13.80	5.12	-11.51	-12.77	10.83	7.34	-2.35
-16.25	12.66	-13.77	5.33	-11.94	-12.66	3.07	10.72	3.35
-13.60	10.50	3.40	1.46	-3.93	-9.31	8.05	-11.00	2.79
19.86	10.20	15.69	-0.68	-10.67	-7.61	10.05	8.55	2.04

Table 3-I Phase Comparison between CAMAC and PDI Algorithms

CAMAC FFT Algorithm Results								
Avg Curr	n = 1	n = 2	n = 3	n = 4	n = 5	n = 6	n = 7	n = 8
5.0	84.55	1816.61	14.96	2.04	0.73	0.41	0.23	0.47
5.0	84.28	1816.73	14.71	1.77	0.57	0.61	0.28	0.59
5.0	82.83	1816.82	14.45	1.23	0.86	0.32	0.38	0.28
5.0	84.41	1817.14	14.68	1.81	0.44	0.57	0.19	0.26
5.0	85.07	1817.43	14.60	2.10	0.68	0.74	0.07	0.75

PDI FFT Algorithm Results								
Avg Curr	n = 1	n = 2	n = 3	n = 4	n = 5	n = 6	n = 7	n = 8
5.0	84.04	1817.33	14.62	1.92	1.00	0.59	0.32	0.39
5.0	84.20	1817.05	14.45	1.92	0.66	0.45	0.39	0.42
5.0	85.84	1817.36	16.11	2.16	0.99	0.60	0.09	0.66
5.0	83.69	1816.81	15.36	1.91	1.18	0.16	0.30	0.34
5.0	84.14	1817.32	15.00	1.77	1.21	0.06	0.37	0.22

CAMAC FFT Algorithm Results								
n = 9	n = 10	n = 11	n = 12	n = 13	n = 14	n = 15	n = 16	n = 17
0.20	0.34	0.23	0.54	0.03	0.21	0.19	0.62	0.60
0.40	0.06	0.39	0.18	0.15	0.38	0.40	0.20	0.23
0.11	0.18	0.35	0.24	0.25	0.11	0.09	0.20	0.34
0.31	0.07	0.34	0.31	0.18	0.26	0.30	0.28	0.38
0.33	0.22	0.42	0.06	0.30	0.20	0.26	0.27	0.41

PDI FFT Function Results								
n = 9	n = 10	n = 11	n = 12	n = 13	n = 14	n = 15	n = 16	n = 17
0.28	0.02	0.30	0.52	0.41	0.25	0.33	0.90	0.46
0.29	0.05	0.26	0.11	0.24	0.14	0.25	0.38	0.35
0.19	0.46	0.37	0.23	0.26	0.50	0.23	0.59	0.36
0.24	0.25	0.13	0.17	0.43	0.25	0.25	0.40	0.34
0.18	0.38	0.18	0.50	0.28	0.37	0.13	0.48	0.23

Table 3-II Amplitude Comparison between CAMAC and PDI Algorithms

The PDI and CAMAC algorithms used to compute the harmonics are shown in Appendix A, Figures A-1 and A-2 respectively.

4 Cycle Analysis

A simulation was completed using System View and MatLab analysis programs to analyze the differences of the continuous and discrete rotation methods, independent of the PDI measurement system. This program was used to generate a ten period waveform, simulating five continuous forward probe rotations, and a two period waveform, simulating one forward probe rotation. An FFT was then conducted on the two data sets. The simulation frequency was set at 10 Hz, sampled at 1000 Hz and the signal set at 1 Volt, with 1% Gaussian noise added. The 1,000 Hz sampling rate is equivalent to the PDI data acquisition rate of 200 samples per revolution.

Fig. 5.2-I shows a two period waveform and the FFT of the average of five, two period cycles. Fig. 5.2-II shows a ten period waveform and the FFT of that waveform.

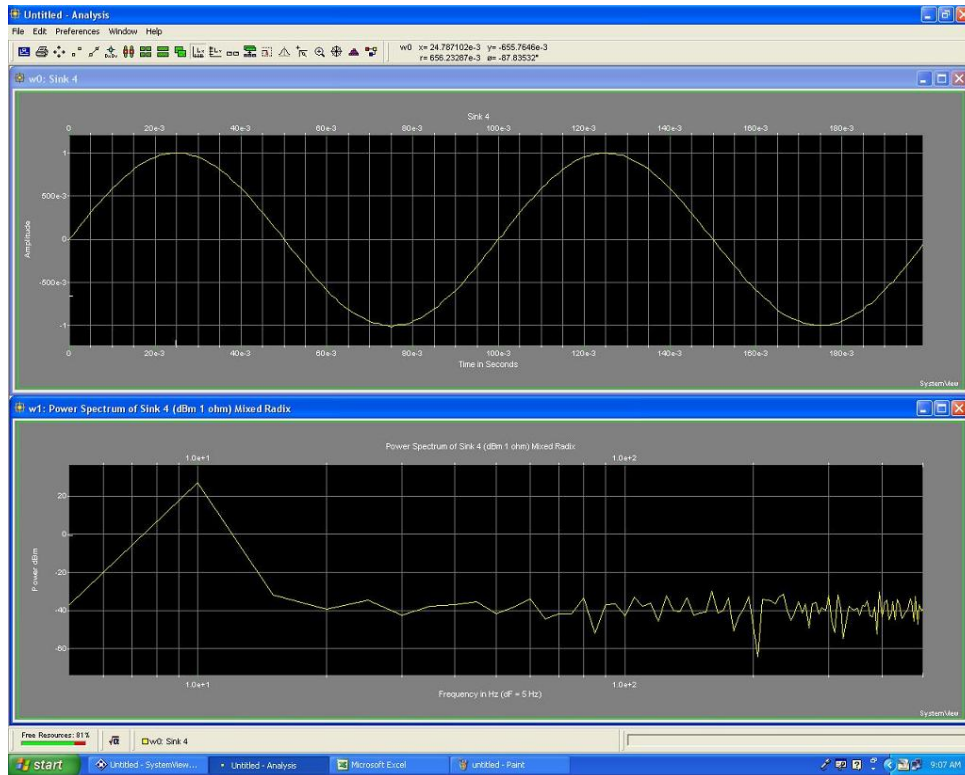


Figure 5-I Average of five Double Cycles

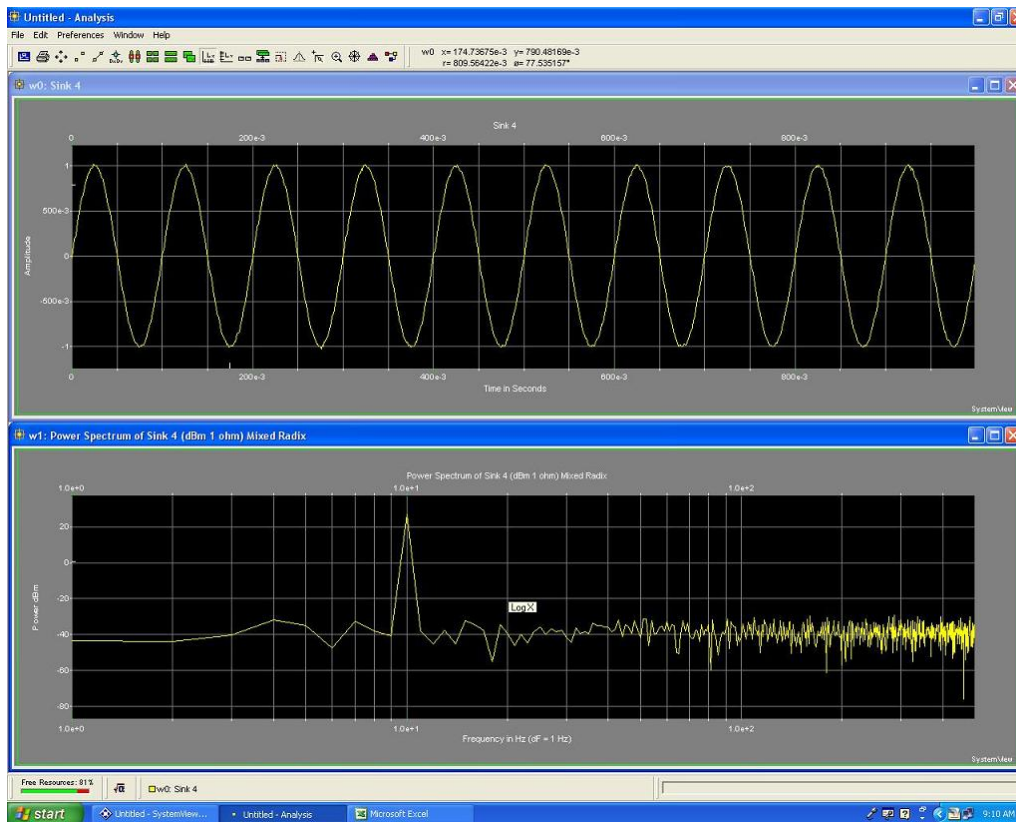


Figure 5-II Five Continuous Cycles

When five continuous cycles were used, the number of frequency intervals increased which resulted in a better frequency resolution. When measuring magnets, a complex waveform is produced by the induced voltage picked up by the rotating probe with the number of samples per revolution corresponds to bins. Spinning the probe continuously provides more bins which, in turn, produces an increasingly accurate representation of the harmonic content of the magnet.

The continuous rotation method produces more zero crossings increasing the ability of the FFT routine to resolve the frequency of the signal. As the number of zero crossings increased, the uncertainty, a consequence of the complexity of the waveform, decreased resulting in a clearer overall representation of the induced signal.

The PDI software used the real and imaginary components calculated by the LabWindows/CVI ReFFT function to extract the desired harmonics. To do this, the real and imaginary values from the FFT data were extracted at multiples of the number of continuous rotations. For example, if the probe was spun for 5 revolutions in a quadrupole magnet, the quadrupole term would correspond to $(n=2) * (5 \text{ revolutions}) = 10$. The function used to determine the harmonic content from the FFT data is shown in Figure 5-III.

```
void vtcoil_calc_vthar(int num_samp, double vtfft_re[], double vtfft_im[],
    int num_rev, int num_har, double vthar_re[], double vthar_im[])
{
    /* The harmonics are at 1, 2, 3, ... cycles per revolution */
    vthar_re[0] = 0.;
    vthar_im[0] = 0.;
    for (i = 1; i <= num_har; i++)
    {
        vthar_re[i] = vtfft_re[i * num_rev];
        vthar_im[i] = vtfft_im[i * num_rev];
    }

    /* Done */
    return;
}
```

Figure 5-III Harmonic Calculation Function

5 Probe Reproducibility Tests

Data was collected on each of the five rotating coil probes used in the Magnet Measurement Facility. The collected data was composed of the average of five discrete forward rotations, similar to the method used in the CAMAC data acquisition system. Data collection in the forward direction only was chosen to eliminate any backlash error induced in the motor to probe linkage.

QB103, a six inch long laminated quadrupole with a two inch bore, was used for each probe measurement. The EPICS control system was used to cycle hysteresis and set the magnet current at five amps at the beginning of each measurement day. The magnet current was monitored over the course of the day to ensure it remained constant. The current was not cycled between measurements, but was only cycled at the beginning of each morning. Table 5-I shows the reproducibility of each probe as a percentage of the amplitude difference over the average amplitude.

Coil 1 Short Probe - 50 turns Outside Coil						
Probe ID	N = 2	Run 1	Run 2	Run 3	Run 4	Run 5
P1A	% Dev from average	0.029%	0.046%	0.041%	0.029%	0.070%
P2A	% Dev from average	0.312%	0.418%	0.215%	0.120%	0.115%
Coil 2 Short Probe - 100 turns inside Coil						
P1A	% Dev from average	0.041%	0.052%	0.056%	0.046%	0.108%
P2A	% Dev from average	0.189%	0.238%	0.095%	0.201%	0.100%
Coil 4 Long Probe						
P1C (100 turns)	% Dev from average	0.063%	0.061%	0.094%	0.041%	0.042%
P2B (90 turns)	% Dev from average	0.147%	0.138%	0.221%	0.217%	0.385%

Table 5-I Probe Reproducibility at 5 amps as a percentage of signal strength QB103

6. Conclusions

System repeatability of the PDI data acquisition unit itself is at a worse 0.05% over periods of four hours or less using a reference signal that mimics a quadrupole magnet. In general system repeatability was found to be at a level better than 0.02%.

Though the repeatability of the measurements done using five discrete rotations was slightly noisier than the repeatability of the measurements done using five continuous rotations at all three coil input locations, in general, the input location of the reference signal, direct connection to the PDI unit or any coil location at the probe junction, did not significantly affect the system repeatability.

Simulations using System View and MatLab suggest better FFT results are obtained using measurement data from five continuous rotations instead of five discrete, averaged rotations.

FFT routines used by the PDI stand are equivalent to routines used in the existing CAMAC stand routine.

Overall system repeatability for the four measurements probes used in the MMF have been measured on a QB magnet at 5 amps and are specified as:

1. P1A – 0.1%
2. P1C – 0.1%
3. P2A – 0.4%
4. P2B – 0.4%

7 Path Forward

To further the commissioning process it should be useful to quantify system performance regarding the five conditions listed below. With the exception of any egregious or otherwise malign system performance in characterizing those conditions, the commissioning process will be concluded. If there are any additional measurements that should be performed to characterize the system, please propose the pertinent measurements and describe the significance of these measurements as it relates to the performance of the system, prior to 1 February 2006.

1. Specify system repeatability using probe P3A (Reference the technote Some UV Quadrupole Measurements)
2. Do probe repeatability using reference signal at each PDI gain (harmonics should not change across gain setting)
 - a. Short Term – less than four hours
 - b. Long Term – less than eight hours
3. Determine optimum number of forward rotations used for data averaging
4. Compare forward and backward averaged probe data to forward only probe data.
5. Do this analysis for coil 3 (bucked: coil1 – coil 2). The repeatability should be no worse than the worst case repeatability for coil 1 or coil 2 listed above.

Appendix A FFT Functions Used For Comparison

```

/* ***** */
/*
 * vtcoil_jlab_fft
 * This function is used to compute the amplitude and phase angle of the
 * voltage samples in the same manner as the JLab CAMAC measurement system.
 *
 * Ken Baggett
 * 9/22/2004
 */
void vtcoil_jlab_fft(double vt[], int num_har, int currentIndex, int coilIndex)
{
    int i, j;
    double dx;
    double* xsum;
    double* ysum;
    double* amplitudes;
    double* phases;
    double pi = 3.1415927;
    double theta = 0.;
    double width = 0.;

    // 1 count every 3.6 degrees for 100 counts
    dx = (360. / vtcoil_param.num_samp_per_rev) * (pi / 180.);

    xsum = (double*) malloc((num_har+1) * sizeof(double));
    ysum = (double*) malloc((num_har+1) * sizeof(double));
    amplitudes = (double*) malloc((num_har+1) * sizeof(double));
    phases = (double*) malloc((num_har+1) * sizeof(double));

    for(i=0; i < num_har; i++)
    {
        xsum[i] = 0.;
        ysum[i] = 0.;
    }

    //printf("\n====VT Coil Readings in uV*S=====\n");

    // convert from V-S to uV-S
    for(i=0; i <= vtcoil_param.num_samp_per_rev; i++)
    {
        vt[i] = vt[i]* 1000000.0;
    }

    // do the integrals
    for(i=0; i <= vtcoil_param.num_samp_per_rev; i++)
    {
        if(i == 0 || i == vtcoil_param.num_samp_per_rev)
        {
            width = dx / 2.;
        }
        else
        {
            width = dx;
        }
        theta = i * dx;
        for(j=0; j < num_har; j++)
        {
            xsum[j] += (vt[i] * cos((j * theta)) * width);
            ysum[j] += (vt[i] * sin((j * theta)) * width);
        }
    }

    // Normalize the integrals and calc Amplitude and Phase
    xsum[0] /= (2. * pi);
    ysum[0] /= (2. * pi);

    amplitudes[0] = xsum[0];
    phases[0] = -90.;

    for(i = 1; i <= num_har; i++)
    {
        xsum[i] /= pi;
        ysum[i] /= pi;

        amplitudes[i] = sqrt (pow(xsum[i], 2.) + pow (ysum[i], 2.));

        if(ysum[i] == 0.)
        {
            printf("Zero Intergal");
            return;
        }

        phases[i] = -(atan2 (xsum[i], ysum[i]) / i);
        phases[i] *= (180. / pi);
    }

    // now store the values for future writeout
    for(i=0; i < num_har; i++)
    {
        fftAmp[i][currentIndex][coilIndex] = amplitudes[i];
        fftPhase[i][currentIndex][coilIndex] = phases[i];
    }
}

```

Figure A-1 CAMAC FFT Algorithm

```

/* ***** */
/*
 * vtcoil_al_tFFT
 * This function is used to compute the amplitude and phase angle of the
 * voltage samples.
 * Amplitude is given by the magnitude of the normal and skew components
 * Phase of each harmonic is given by the angle of the harmonic normalized to
 * the period.
 *
 * Ken Baggett
 * 10/25/2005
 */

void vtcoil_al_tFFT(double vthar_re_ave[], double vthar_im_ave[], int num_har, int currentIndex, int
coilIndex, int num_str_har)
{
    int i;
    double amplitudes[50];
    double phases[50];
    double temp;

    amplitudes[0] = 0.0;
    phases[0] = -90.;
    fftAmp[0][currentIndex][coilIndex] = amplitudes[0];
    fftPhase[0][currentIndex][coilIndex] = phases[0];

    // now store the values for future writeout
    for(i=1; i <= num_har; i++)
    {
        // Calculate the harmonic strength
        amplitudes[i] = sqrt( pow(vthar_re_ave[i], 2) + pow(vthar_im_ave[i], 2) );
        amplitudes[i] *=1000000.0;

        // Calculate the south pole angle
        phases[i] = - (atan2(vthar_im_ave[i], vthar_re_ave[i]) + 3.1415927 / 2) / i;

        if (phases[i] > 3.1415927 / i)
            phases[i] = phases[i] - 2. * 3.1415927 / i;
        if (phases[i] < -3.1415927 / i)
            phases[i] = phases[i] + 2. * 3.1415927 / i;

        // Convert the south pole angle to degrees
        phases[i] = phases[i] * 180. / 3.1415927;

        fftPhase[i][currentIndex][coilIndex] = phases[i];
        fftAmp[i][currentIndex][coilIndex] = amplitudes[i];
    }
}

```

Figure A-2 PDI FFT Algorithm

Appendix B N = 2 Amplitude Data for Each Coil Location

Measurement #	Coil 1 (uV*Sec)				
	P2A	P2A	P2A	P2A	P2A
	5 Cycles	5 Cycles	5 Cycles	5 Cycles	5 Cycles
	Forward Only	Forward Only	Forward Only	Forward Only	Forward Only
	PRP2A011.fft	PRP2A012.fft	PRP2A013.fft	PRP2A014.fft	PRP2A015.fft
1	14457.520	8217.441	8240.319	8233.880	8234.836
2	14427.982	8214.719	8222.648	8235.853	8231.632
3	14464.659	8205.696	8223.235	8233.454	8231.822
4	14440.012	8214.880	8231.669	8236.777	8235.318
5	14422.583	8209.382	8236.182	8228.210	8227.317
6	14425.431	8209.819	8236.914	8234.438	8232.204
7	14439.798	8216.783	8236.992	8227.038	8233.455
8	14444.892	8197.769	8235.400	8231.942	8236.806
9	14437.822	8232.071	8224.809	8226.901	8231.007
10	14467.625	8205.618	8230.126	8230.144	8234.465
Average	14442.8324	8212.4178	8231.8294	8231.8637	8232.8862
Min	14422.5830	8197.7690	8222.6480	8226.9010	8227.3170
Max	14467.6250	8232.0710	8240.3190	8236.7770	8236.8060
Difference	45.04200	34.30200	17.67100	9.87600	9.48900
% Deviation	0.312%	0.418%	0.215%	0.120%	0.115%

Measurement #	Coil 2 (uV*Sec)				
	P2A	P2A	P2A	P2A	P2A
	5 Cycles	5 Cycles	5 Cycles	5 Cycles	5 Cycles
	Forward Only	Forward Only	Forward Only	Forward Only	Forward Only
	PRP2A016.fft	PRP2A017.fft	PRP2A018.fft	PRP2A022.fft	PRP2A023.fft
1	8171.222	8168.985	8172.499	8164.141	8174.368
2	8171.141	8165.879	8169.573	8165.550	8173.341
3	8155.819	8165.739	8171.299	8166.825	8172.813
4	8157.134	8166.342	8169.731	8173.038	8173.417
5	8158.787	8166.219	8168.465	8170.707	8167.962
6	8158.499	8161.559	8170.338	8166.661	8168.707
7	8160.852	8166.035	8168.911	8163.027	8168.187
8	8156.466	8157.513	8170.029	8177.142	8169.501
9	8161.070	8176.934	8166.266	8160.686	8168.171
10	8162.886	8172.542	8174.057	8167.355	8166.161
Average	8161.3876	8166.7747	8170.1168	8167.5132	8170.2628
Min	8155.8190	8157.5130	8166.2660	8160.6860	8166.1610
Max	8171.2220	8176.9340	8174.0570	8177.1420	8174.3680
Difference	15.40300	19.42100	7.79100	16.45600	8.20700
% Deviation	0.189%	0.238%	0.095%	0.201%	0.100%

	Coil 1 (uV*Sec)				
	P1A	P1A	P1A	P1A	P1A
	5 Cycles	5 Cycles	5 Cycles	5 Cycles	5 Cycles
	Forward Only	Forward Only	Forward Only	Forward Only	Forward Only
Measurement #	PRP1A001.fft	PRP1A002.fft	PRP1A003.fft	PRP1A004.fft	PRP1A005.fft
1	1816.150	1816.463	1816.206	1817.141	1816.357
2	1816.374	1816.353	1815.885	1816.717	1816.101
3	1816.633	1816.667	1816.024	1816.782	1816.236
4	1816.672	1816.001	1815.899	1816.914	1816.634
5	1816.644	1816.279	1816.315	1816.726	1816.301
6	1816.342	1816.048	1816.621	1816.619	1815.653
7	1816.450	1816.027	1816.120	1816.666	1815.631
8	1816.191	1816.197	1816.200	1816.663	1815.369
9	1816.540	1815.902	1816.285	1817.144	1816.493
10	1816.328	1815.838	1815.926	1816.711	1816.296
Average	1816.4324	1816.1775	1816.1481	1816.8083	1816.1071
Min	1816.1500	1815.8380	1815.8850	1816.6190	1815.3690
Max	1816.6720	1816.6670	1816.6210	1817.1440	1816.6340
Difference	0.52200	0.82900	0.73600	0.52500	1.26500
% Deviation	0.029%	0.046%	0.041%	0.029%	0.070%

	Coil 2 (uV*Sec)				
	P1A	P1A	P1A	P1A	P1A
	5 Cycles	5 Cycles	5 Cycles	5 Cycles	5 Cycles
	Forward Only	Forward Only	Forward Only	Forward Only	Forward Only
Measurement #	PRP1A006.fft	PRP1A007.fft	PRP1A008.fft	PRP1A009.fft	PRP1A010.fft
1	1750.485	1750.861	1751.639	1751.520	1751.667
2	1750.531	1751.595	1751.979	1751.983	1751.454
3	1750.155	1751.467	1751.572	1751.938	1750.817
4	1750.803	1751.253	1751.538	1751.767	1750.466
5	1750.392	1751.611	1751.346	1751.242	1750.679
6	1750.160	1751.630	1751.318	1751.861	1751.419
7	1750.149	1751.777	1751.502	1751.925	1750.404
8	1750.192	1751.596	1751.353	1751.940	1749.774
9	1750.082	1751.353	1751.598	1752.048	1750.906
10	1750.365	1751.203	1750.993	1751.932	1750.550
Average	1750.3314	1751.4346	1751.4838	1751.8156	1750.8136
Min	1750.0820	1750.8610	1750.9930	1751.2420	1749.7740
Max	1750.8030	1751.7770	1751.9790	1752.0480	1751.6670
Difference	0.72100	0.91600	0.98600	0.80600	1.89300
% Deviation	0.041%	0.052%	0.056%	0.046%	0.108%

Coil 4 (uV*Sec)					
	P2B	P2B	P2B	P2B	P2B
	5 Cycles				
	Forward Only				
Measurement #	PRP2B001.fft	PRP2B002.fft	PRP2B003.fft	PRP2B004.fft	PRP2B005.fft
1	18789.212	18771.829	18772.203	18765.126	18767.200
2	18761.696	18770.157	18768.459	18750.299	18769.684
3	18764.149	18756.591	18779.026	18755.136	18771.466
4	18781.217	18759.289	18770.494	18765.736	18762.874
5	18773.138	18772.288	18772.659	18762.051	18781.481
6	18764.773	18766.121	18778.973	18745.686	18789.627
7	18768.116	18775.149	18737.560	18786.321	18747.359
8	18770.797	18764.202	18760.130	18761.813	18757.169
9	18780.203	18770.462	18768.927	18756.482	18719.624
10	18767.085	18782.459	18752.353	18762.011	18717.387
Average	18772.0386	18768.8547	18766.0784	18761.0661	18758.3871
Min	18761.6960	18756.5910	18737.5600	18745.6860	18717.3870
Max	18789.2120	18782.4590	18779.0260	18786.3210	18789.6270
Difference	27.51600	25.86800	41.46600	40.63500	72.24000
% Deviation	0.147%	0.138%	0.221%	0.217%	0.385%

Coil 4 (uV*Sec)					
	P1C	P1C	P1C	P1C	P1C
	5 Cycles				
	Forward Only				
Measurement #	PRP1C001.fft	PRP1C002.fft	PRP1C003.fft	PRP1C004.fft	PRP1C005.fft
1	4921.630	4921.423	4921.237	4923.656	4923.824
2	4920.738	4922.893	4920.726	4924.291	4924.298
3	4921.121	4923.679	4923.079	4924.048	4924.220
4	4921.692	4923.373	4924.365	4925.659	4924.031
5	4921.000	4924.418	4924.255	4924.703	4924.183
6	4923.179	4924.171	4923.671	4924.551	4923.314
7	4923.005	4924.223	4924.124	4925.271	4924.210
8	4921.997	4922.944	4924.594	4924.744	4923.995
9	4923.822	4923.932	4924.606	4923.847	4922.220
10	4923.482	4923.653	4925.336	4923.952	4922.471
Average	4922.1666	4923.4709	4923.5993	4924.4722	4923.6766
Min	4920.7380	4921.4230	4920.7260	4923.6560	4922.2200
Max	4923.8220	4924.4180	4925.3360	4925.6590	4924.2980
Difference	3.08400	2.99500	4.61000	2.00300	2.07800
% Deviation	0.063%	0.061%	0.094%	0.041%	0.042%